American Mineralogist, Volume 94, pages 27–33, 2009

Color origin and heat evidence of paleontological bones: Case study of blue and gray bones from San Josecito Cave, Mexico

Céline Chadefaux,[1] Colette Vignaud,[1] Emilie Chalmin,[2] Jasinto Robles-Camacho,[3] Joaquin Arroyo-Cabrales,[4,5] Eileen Johnson,[5] and Ina Reiche[1,*]

[1]Laboratorie du Centre de Recherche et de Restauration des Musées de France (LC2RMF), UMR 171 CNRS, 75001 Paris, France
[2]ID21, European Synchrotron Research Facility (ESRF), 38043 Grenoble, France
[3]Laboratorio de Arqueometría del Occidente, Centro INAH Michoacán, Instituto Nacional de Antropología e Historia, Morelia, Michoacán 58000, Mexico
[4]Laboratorio de Arqueozoología, Subdirección de Laboratorios y Apoyo Académico, Instituto Nacional de Antropología e Historia, México, Distrito Federal 06060, Mexico
[5]Museum of Texas Tech University, Lubbock, Texas 79409-3191, U.S.A

Abstract

Results of the investigation of paleontological blue and gray bone fragments of small vertebrates coming from stratigraphic layer 770 at San Josecito Cave (Nuevo Leon, Mexico, dating between 28 000 and 19 000 years BP), are presented. Structural and elemental analyses combining X-ray diffraction (XRD), Fourier-transform infrared spectroscopy (FT-IR), transmission electron microscopy (TEM), and particle-induced X-ray and γ-ray emission (micro-PIXE/PIGE), as well as spectroscopic investigations [i.e., UV/visible/near-IR reflectance spectroscopy and X-ray absorption near-edge structure (XANES) spectroscopy] were performed to identify precisely the origin of the blue stain.

Prior research has shown that Mn^{5+} in tetrahedral coordination could be responsible for the turquoise blue color in mastodon ivory some tens of million years old that was modified by a heat process. Manganese is present in the anionic form of $(MnO_4)^{3-}$ and partially substitute for $(PO_4)^{3-}$ in the hydroxyapatite matrix.

The spectroscopic data of the present study have revealed a heat-induced modification, revealed traces of Mn among the typical bone constituents (Ca, P, Sr, Zn), and provided insights into the color origin of the blue paleontological bones from San Josecito Cave. Cations of Mn^{5+} in a tetrahedral environment of four O^{2-} ions in the apatite structure are found in these bones, the same color origin as in the blue mastodon ivory. As indicated by XANES, Mn^{4+} ions in octahedral coordination as in pyrolusite are found in gray bones. The presence of submicroscopic Mn oxide inclusions might explain the color of the San Josecito gray bones. The formation of Mn^{5+} very likely is induced by heat treatment of the bones under oxidizing conditions. The heat-induced modification of both types of paleontological bones also is indicated by the direct observation of apatite crystals using TEM. The question remains, however, how the heat originated inside the cave.

Keywords: Paleontological blue bone, TEM, XANES, color origin, Mn^{5+} apatite, heat-induced recrystallization

Introduction

Bone and similar materials, including ivory and antler, have an important place in natural history as they record a wealth of information concerning past ways of life (paleodiets, migration, climates) in the form of changes in their aspect and structure as well as in their chemical and isotopic composition. They exhibit a high degree of hierarchy and are a composite material consisting of a nanocrystalline mineral phase [carbonate hydroxyapatite (carb-HAP), $Ca_{10}(PO_4)_{6-x}(CO_3)_xOH$] embedded in an organic matrix (mainly type I collagen).

Bones with blue and green coloration currently have been recovered from paleontological localities and archaeological sites. It is crucial to understand the origin of the blue color to provide a clue about depositional conditions and past environments. The origin of color, however, generally is a subject of controversy (Weiner et al. 1998; Robles et al. 2002; Michel et al. 2006), even if it is clear that a relation exists with heating (intentional or accidental). Indeed, the detection of a heating process is of first importance as an indicator of fire. Very few clear markers exist that provide evidence of fire at a paleontological locality or very early archaeological site.

The first unambiguous evidence for the origin of blue color of ancient bone material was based on research on fossil ivory (Reiche et al. 2000, 2001, 2002a) in the case of "Odontolite." Odontolite is a turquoise imitation made of fossil ivory mate-

* E-mail: ina.reiche@culture.gouv.fr

rial that comes basically from Southern France from paleontological deposits that date to the Miocene (13–16 Ma). It was used in the Middle Ages to decorate metallic art and religious objects. The turquoise blue stain comes from the tetrahedral $(MnO_4)^{3-}$ oxocomplex of Mn^{5+} in ivory apatite. The anionic form of $(MnO_4)^{3-}$ partially substitutes for $(PO_4)^{3-}$ in the hydroxyapatite matrix of ivory. This ion is formed by an oxidation (induced by heating) of Mn^{2+} whose presence in fossil ivory material is due to diagenetic or fossilization processes (Reiche et al. 2000, 2001). Tetrahedral Mn^{5+} ions also have been proposed to explain the turquoise color of bone beads from the Neolithic site of Tell El-Kerkh in Syria. This cause, however, could not be demonstrated directly (Taniguchi et al. 2002). The existence of Mn^{5+} in apatites already is quite well established (Yubao et al. 1993; Mayer et al. 2003).

This case study presents an example of blue coloration of paleontological bone coming from Mexico, within a different context. Fragments of blue and gray bones were excavated from San Josecito Cave (Nuevo Leon, Mexico) (Fig. 1) (Arroyo-Cabrales et al. 1998). The blue fragments belong to stratum 770. They previously have been analyzed (Robles et al. 2002) by X-ray diffraction and energy-dispersive X-ray (EDX) techniques, X-ray fluorescence spectrometry (XRFS), instrumental neutron activation analysis (INAA), scanning electron microscopy with X-ray analysis (SEM-EDX), inductively coupled plasma spectrometry (ICPS), and colorimetric methods. Those analyses, however, have not identified the exact origin of the blue coloration because the potential coloring element, Mn, was not investigated.

New results based on complementary investigations are presented here and provide evidence of heat-induced changes and of Mn-related color origin of the blue and grayish colored bones. The latter investigations especially are based on the following: (1) observation of crystal sizes and shapes by means of transmission electron microscopy (TEM-EDX); (2) elemental analyses by means of micro particle-induced X-ray and γ-ray emission (micro-PIXE/PIGE) allowing determination of the chemical composition between the elements F and U at the major, minor, and trace level; (3) visible/near-IR reflectance spectroscopy (Vis/NIR); and (4) X-ray absorption near-edge structure (XANES) spectroscopy at the Mn *K*-edge.

Material

San Josecito Cave is located southwest of Aramberri (24° 06' N, 99° 49' W; 2250 m elevation), in the municipality of Zaragoza, Nuevo León, on the western flank of the Sierra Madre Oriental. The cave is a single-drop, multi-entrance fissure that occurs in folded Late Jurassic or Early Cretaceous limestone. All three now-open natural entrances descend vertically 12 to 30 m to the main chamber or to a sloping tunnel into this room. A horizontal or walking entrance apparently never existed. The main chamber is 34 m long and 25 m wide. The fossil fauna is composed of mollusks, amphibians, reptiles, birds, and mammals, including more than 30 extinct species (Arroyo-Cabrales et al. 1998). These remains have been radiocarbon-dated to an interval of

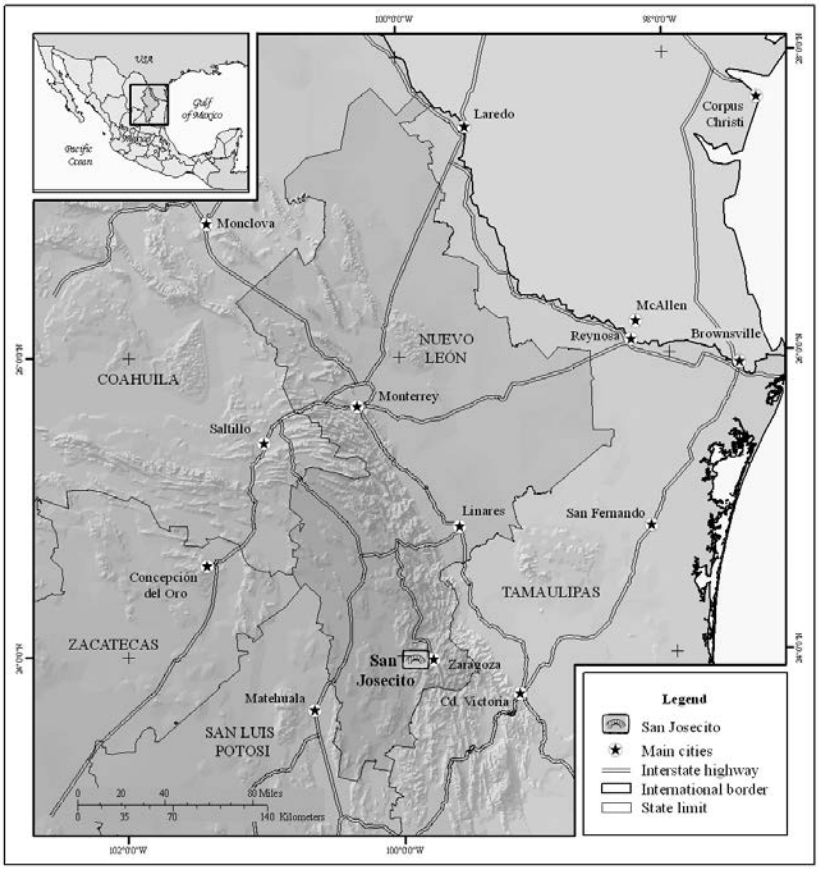

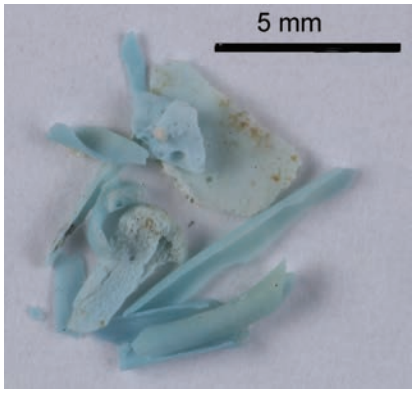

Figure 1. Location of San Josecito Cave, Nuevo León, México. Blue bone fragments from stratum 770.

time between 44 000 and 19 740 years BP and specifically those from stratum 770 between 28 000 and 19 740 years BP (Arroyo-Cabrales et al. 1998; Gonzalez et al. 2003).

Materials from one very thin stratigraphic unit (770), above the 28 000 year BP old unit 720, showed a very characteristic blue-greenish stain. The stratum 770 sample was composed of small vertebrate bones, including those of lizards (*Barisia imbricata*), bats (*Desmodus rotundus*, *Leptonycteris* sp.), and rodents (*Neotoma* sp., *Peromyscus* sp.). Some bones were compressed strongly, probably due to sediment load (Robles et al. 2002). Most bones were stained completely, including the overall shaft. A subsample of the blue bone fragments was chosen for analysis (~10 g), mostly pertaining to rodents (Fig. 1). From those, a couple of fragments were assayed; one having a blue stain and the other a gray stain.

Sample preparation and analytical methods

Bone powder was prepared by grinding a small fragment of each sample in an agate mortar. A KBr pellet was prepared from a small powder fraction for FT-IR spectroscopy. Another powder fraction was diluted in ethanol and deposited on a carbon coated-copper grid for TEM. This preparation was necessary to obtain crystals thin enough to be transparent under the electron beam. No special preparation procedure was necessary for external beam microPIXE/PIGE, XANES, and Vis/NIR spectroscopy.

Analysis of vibrational bands in FT-IR spectra enabled the identification of crystalline and amorphous phases of the sample. Measurements were carried out with a Perkin Elmer Spectrum 2000 spectrometer in transmission mode at the LC2RMF. Ten scans were collected at a resolution of 4 cm^{-1} for each analysis. The splitting factor (SF), a criterion usually determined on ancient bone to estimate its apatite crystallinity, was measured from phosphate absorption bands 603 and 565 cm^{-1} as described by Weiner et al. (1990).

XRD measurements were carried out on bone powder in locked coupled scan mode with a Bruker D5000 diffractometer using Co$K\alpha$ radiation. Analysis was performed during 48 h with a step size of 0.04° and a time per step of 1 s between 10 and 90° to identify phases and to calculate the crystallinity index (CI) of the samples from the full-width at half maximum (FWHM) of the (002) apatite line (Tuross et al. 1989).

TEM observations were carried out on a 200 kV Jeol transmission electron microscope equipped with a Link Isis energy-dispersive X-ray analysis system (EDX). In addition, selected area electron diffraction (SAED) was applied to identify the crystal structures (Leventouri 2006).

The chemical composition of the bone fragments was determined by micro-PIXE/PIGE using the external micro-beam line at the tandem particle accelerator AGLAE (Accélérateur Grand Louvre d'Analyse Elémentaire, Paris, France) installed at the LC2RMF. Measurements were undertaken in a He atmosphere. The accelerator facility is described in detail by Calligaro et al. 2004. Spectrum evaluation by means of the GUPIX software (described by Maxwell et al. 1988) permitted calculation of elemental concentrations and statistical errors of the micro-PIXE measurements. Simultaneous micro-PIGE measurements were carried out to quantify the F content of the samples. The quantitative evaluation of PIGE spectra was based on the simultaneous analysis of appropriate reference samples (Reiche et al. 2003).

Diffuse reflectance spectra were measured at room temperature between 200 and 2500 nm with a spectral resolution between 0.04 and 0.4 nm using a CARY 5 UV-visible-near IR spectrophotometer on untreated samples. A blank (Halo) was measured prior to acquisition of each spectrum.

Spatially resolved Mn *K*-edge XANES spectra for model compounds and the paleontological samples were collected under high-resolution conditions (~0.5 eV) at the ID21 beamline at the European Synchrotron Radiation Facility (ESRF, Grenoble, France) using an Si(220) double-crystal monochromator (Susini et al. 2002). This method provided information on the valence state and on the chemical environment of the target element. Pre-edge and main-edge features were collected with a resolution of 0.4 eV steps. The spot size of the beam was fixed by a pinhole of 200 µm diameter. Energy was calibrated (±0.05 eV) using reference compounds: Mn metal foil and $KMnO_4$. The XANES spectra were acquired in fluorescence mode using a Silicon Drift Detector (SDD). A Kapton filter (128 µm) was added in front of the snout of the detector to cut the lower energy part of the XRF spectra and thus avoid detector saturation due to the high Ca concentration. XANES spectra were normalized in intensity using conventional methods (a combination of polynomial and spline functions as available in the XAFS package; Winterer 1997).

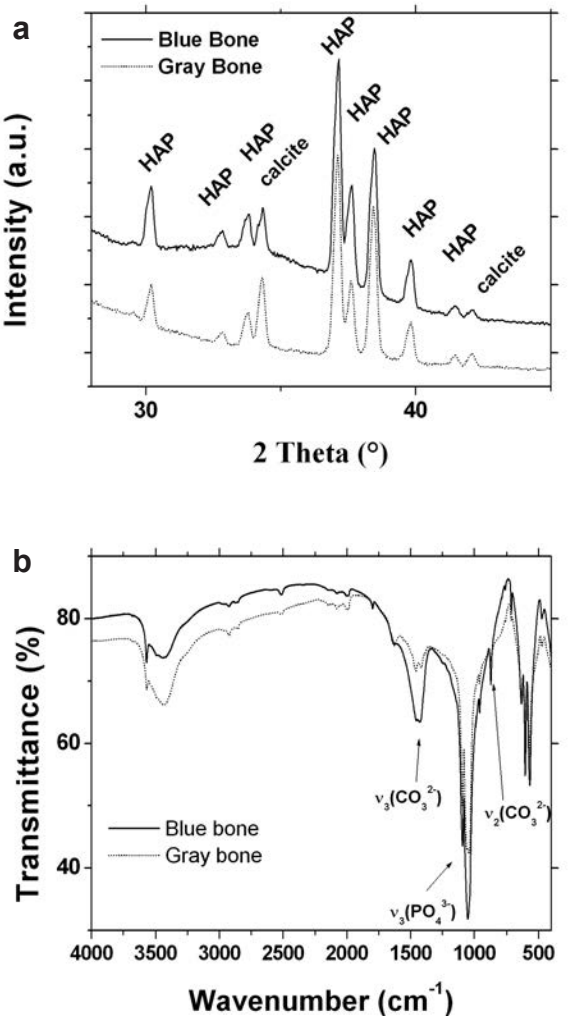

Figure 2. (**a**) XRD diagrams (Co$K\alpha$ source), HAP = Hydroxyapatite, (**b**) FT-IR spectra of blue bone and gray bone.

Results

Structure of bone fragments

XRD results revealed that both samples are composed principally of carbonate hydroxyapatite (JCPDS 09-0432) and calcite (JCPDS 005-0586) (Fig. 2a). FT-IR analysis indicated that organic matter as expected for bone was not detected (Fig. 2b). Table 1 summarizes the calculated crystallinity index (CI) measured by XRD, the splitting factor (SF) calculated from FT-IR spectroscopy for the hydroxyapatite main phase, and the secondary phases observed in the samples. An estimation of the carbonate content calculated by the ratio of the intensities of the ν_2 carbonate vibration vs. the ν_3 phosphate vibration band ($I[\nu_2(CO_3^{2-})]/I[\nu_3(PO_4^{3-})]$) measured by FT-IR and noted C/P was included in Table 1. The crystallinity index measured by XRD

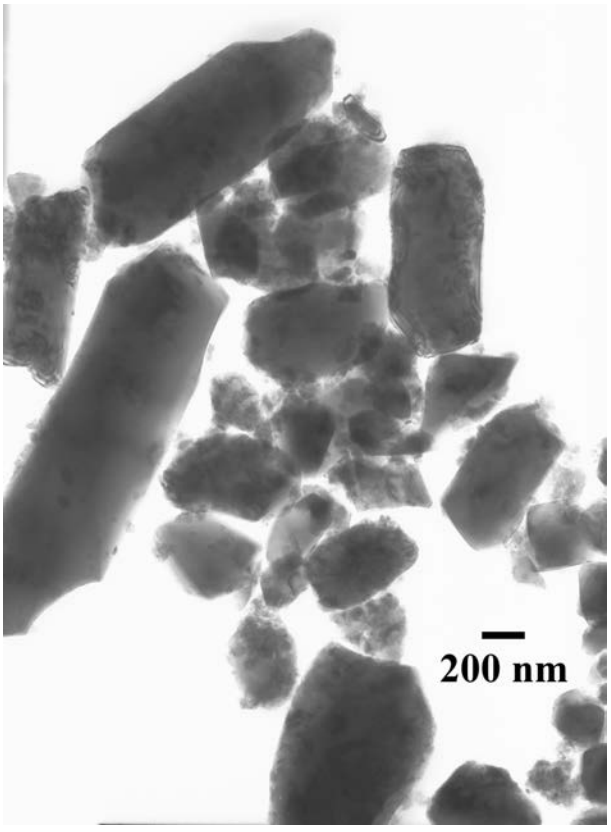

FIGURE 3. TEM micrograph of gray bone showing several crystals indicating the size heterodispersity.

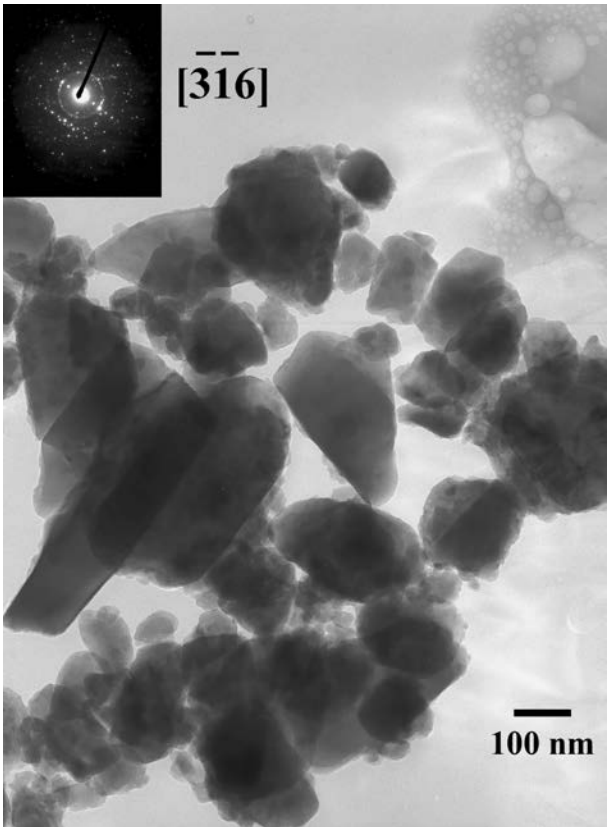

FIGURE 4. TEM micrograph with SAED of blue bone showing several crystals indicating an important size heterodispersity.

TABLE 1. Characteristics of the paleontological bone samples compared to a modern one

	Crystallinity index (CI) (XRD)	Splitting factor (SF) (FT-IR)	Index related to the carbonate content (C/P)	Secondary phases
Blue bone	0.23 ± 0.01	4.4 ± 0.1	0.73 ± 0.03	calcite
Gray bone	0.25 ± 0.01	4.8 ± 0.1	0.57 ± 0.03	calcite
Modern bone	0.47 ± 0.03	2.7 ± 0.1	0.38 ± 0.03	–

of the blue sample was low (about 0.24) and the splitting factor measured by FT-IR spectroscopy is high (about 4.6) compared to the modern bone. Modern bone showed a mean CI of 0.47 ± 0.03 and a mean SF of 2.7 ± 0.1. In addition, TEM observations showed large polygonal apatite crystals and irregular platelets (Figs. 3 and 4). Their size reached up to 2500 nm for the gray bone and up to 500 nm for the blue bone samples. The morphology and crystal size were altered considerably in comparison to that of modern bone showing a mean grain size of 10 nm long (Reiche et al. 2002b).

Chemical composition of the bones

Table 2 summarizes the chemical compositions of blue, gray, and modern bones measured by micro-PIXE/PIGE. These values show that Ca is enriched slightly in the gray paleontological bone compared to the modern reference, whereas P is more concentrated in the blue bone than in the modern and the gray paleontological bone. Magnesium and Na in the ancient bones have lower concentrations than in modern bone. Strontium, S, Fe, Mn, Cu, and F have higher concentrations in the ancient bones compared to modern reference. Only the Zn content in blue bone is found to be lower than in the modern reference. When comparing the Ca, Na, Mg, Cl, Sr, Fe, Cu, and Zn contents of the gray to the blue paleontological bone, they are higher in

TABLE 2. Mean element concentrations and ranges (obtained with the statistical error for each element) detected by microPIXE-PIGE in the paleontological and modern bone samples

Elemental content (ppm)	Modern calf bone	Blue bone	Gray bone
Ca	410 000 ± 500	390 000 ± 660	411 000 ± 450
P	176 000 ± 350	179 500 ± 450	173 000 ± 350
Mg	5500 ± 150	1450 ± 250	2100 ± 130
Si	–	–	–
Na	8000 ± 240	–	6100 ± 260
Cl	1000 ± 60	–	2500 ± 68
Sr	–	50 ± 5	140 ± 10
S	1400 ± 100	4150 ± 150	3370 ± 100
Fe	–	40 ± 4	680 ± 14
Cu	–	60 ± 3	300 ± 7
Zn	120 ± 5	90 ± 3	2000 ± 16
Mn	–	150 ± 6	70 ± 9
F	–	1100	300

Note: Dash = below the detection limit.

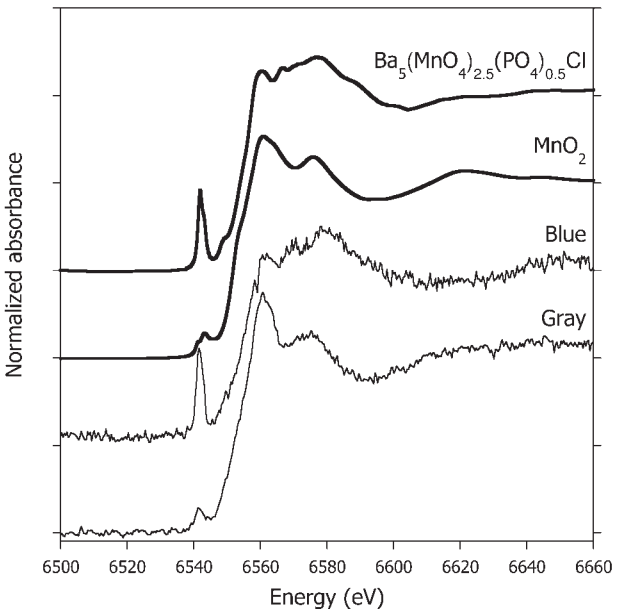

FIGURE 5. Manganese *K*-edge XANES spectra of reference compounds $Ba_5(MnO_4)_{2.5}(PO_4)_{0.5}Cl$ and MnO_2 (pyrolusite) and of blue and gray bone from San Josecito Cave.

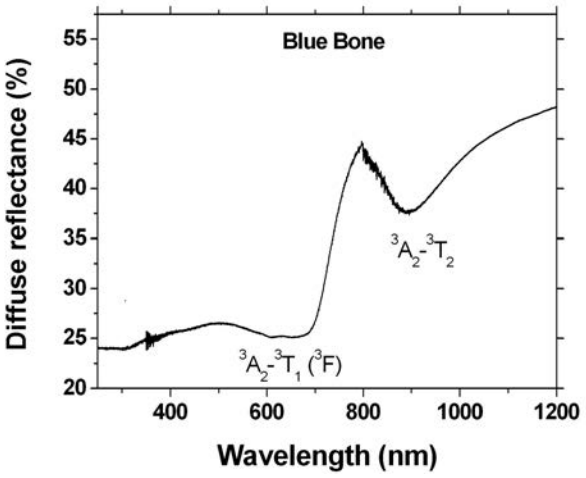

FIGURE 6. Diffuse reflectance spectra between 250 and 1200 nm of blue bone.

the gray bone, whereas Mn, F, and S concentrations are higher in the blue one.

Speciation of Mn

XANES measurements at the Mn *K*-edge were performed to clarify the Mn oxidation state in the bone fragments. By comparison of the Mn *K*-edge XANES spectrum with the reference spectra from a series of Mn oxihydroxides and synthetic compounds, it was possible to recognize the feature of a pyrolusite phase (MnO_2) for the gray bone (Fig. 5). The XANES feature of the blue bone, however, corresponded to a more oxidized reference, i.e., $Ba_5(MnO_4)_{2.5}(PO_4)_{0.5}Cl$ (Fig. 5).

The position of the pre-edge peak confirms that the Mn ions in the blue bone correspond to a compound with an oxidized valence state (Mn^{5+}, Fig. 5) while it confirms the presence of Mn^{4+} as pyrolusite, MnO_2, in the gray bone. The intensity of the pre-edge is linked with the coordination. The most intense pre-edge feature corresponds to a tetrahedral environment as observed for the blue bone, and the less intense pre-peak to a more centro-symmetric coordination, e.g., an octahedral environment. The area of the pre-edge of the gray bone is somewhat enhanced compared to that of the regular octahedral MnO_2 structure. Therefore, Mn in the gray bone apparently is in a slightly distorted octahedral coordination.

A diffuse Vis/NIR reflectance spectrum of the blue bone is given in Figure 6. It evidences an electronic transition at 649 nm. Among the spin allowed transitions [$^3A_2 \rightarrow {}^3T_2$, $^3A_2 \rightarrow {}^3T_1(^3F)$, $^3A_2 \rightarrow {}^3T_1(^3P)$] of Mn^{5+} corresponding to $3d^2$ state, only one transition [$^3A_2 \rightarrow {}^3T_1(^3F)$] corresponds to an energy in the visible range (Reinen et al. 1986; Dardenne et al. 1999). It is the transition $^3A_2 \rightarrow {}^3T_1(^3F)$ giving rise to the absorption band at 649 nm that is responsible for the blue coloration.

DISCUSSION

Evidence of heat-induced modification of the bone fragments

TEM micrographs reveal apatite crystals in both paleontological bone fragments that are at least two orders of magnitude larger than those of modern bone. In the gray bone, the crystals (up to 2500 nm) are about 5× larger than in the blue bone fragment (500 nm) and about 200× larger than modern unheated bone (about 10 nm long). Indeed, TEM images (Figs. 3 and 4) show the presence of large-sized apatite crystals with different shapes (rectangular or hexagonal) characteristic of recrystallized bone apatite induced by heat treatment. This increase in grain size at the nanometric scale during heating has been documented in previous studies on ancient bone and ivory (Reiche et al. 2000, 2007). The heating to temperatures above 550 °C (intentional or accidental) of bone samples causes significant apatite crystal growth (Reiche et al. 2002b, 2007). These observations are correlated with the change of more global macroscopic values of SF as shown in Figure 7. Rectangular symbols in Figure 7 represent the mean apatite crystal size measured by TEM, whereas ellipsoids indicate the variation of crystal size observed for a given temperature. Triangles show the SF calculated on the basis of the FT-IR spectrum of the bone at the given temperature. In the case of modern bone, the SF and the apatite crystal size are directly correlated as a function of the temperature.

XANES results, furthermore, indicate the presence of Mn^{4+} ions in the form of pyrolusite, MnO_2, in the gray bone. If the gray bone was heated after the formation of Mn oxides during the fossilization process, the type of Mn oxide also can be used as a temperature indicator. Chalmin et al. (2008) have shown that different Mn oxides are formed as a function of the heating temperature. If the gray bone was heated above 600 °C, XANES analysis would have shown bixbyite. Pyrolusite changes into bixbyite at temperatures higher than 600 °C. Therefore, the gray bone has not been heated above 600 °C if this Mn oxide phase was present before the heating process.

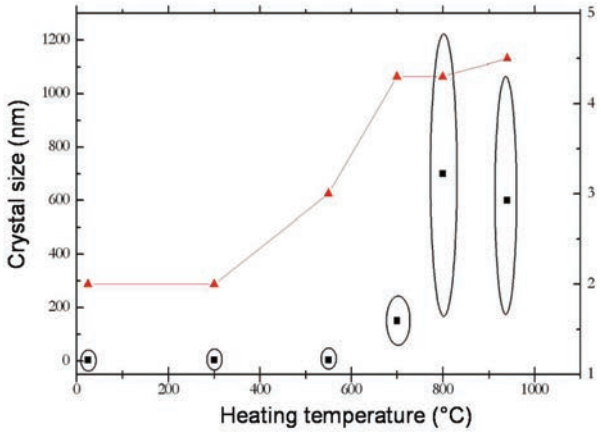

FIGURE 7. Evolution of crystal size and splitting factor during heating of modern bone. Full triangles indicate splitting factors measured by FT-IR [SF(IR)], full squares the average crystal sizes observed by TEM, and ellipsoids the range of the observed crystal sizes (Reiche et al. 2000, 2007).

Origin of the bone coloration

The blue coloration of the bone fragments from San Josecito Cave originates from traces of Mn^{5+} in tetrahedral coordination in the form of $(MnO_4)^{3-}$ that substitute in the apatite structure on some $(PO_4)^{3-}$ sites of the heated bones. In contrast, the gray color is induced by the presence of Mn^{4+} in slightly distorted octahedral coordination as found, e.g., in pyrolusite (MnO_2). This situation suggests that the color is not intrinsic to the apatite phase in the gray bone. The presence of sub-microscopic inclusions of Mn oxide seems most likely. Formation of various Mn oxides in archaeological and paleontological bone during burial is quite common (Reiche et al. 2000; Reiche and Chalmin 2008). These black Mn oxides could be formed by several processes in the soil including the uptake of Mn^{2+} followed by their oxidation and precipitation as oxide or formation induced by bacterial activity. It is not possible to determine exactly when the detected heat process of the bones took place. If it took place after the formation of Mn oxides, it could induce a change in the type of the Mn oxide found in the gray paleontological bones. It is, however, also possible that the Mn oxide inclusions were formed by diagenetic processes that modified the bones during burial and after the heat-induced changes.

In the blue specimen, the heating under oxidizing conditions has induced a transformation of $Mn^{2+, 3+, \text{or } 4+}$ ions into Mn^{5+} ions. The chemical analysis of the bone samples shows that the blue bone is characterized by a higher Mn content compared to the gray one. The Mn concentration, however, is not the determining factor for the coloring effect and the exact reason why the blue color can appear on archaeological and paleontological bone after heating could not be clarified. The color appearance could be linked to the heating temperature but also to the heating time. Gray bones show much larger crystals than blue ones. This situation could be explained by either a higher temperature or a longer exposure to heating. According to previous studies (Reiche et al. 2002b, 2007), an optimal temperature range for the blue color formation in ancient bone and ivory apparently is above 500 °C and below 600 °C. This phenomenon, however, cannot be explained in detail. Further experiments are necessary to clarify this issue.

In any case, the formation of mixed crystals of $Ca_5(PO_4)_{3-x}(MnO_4)_xOH$ with the apatite structure in bone needs, above all, an excess of Ca^{2+} beyond a Ca/P-ratio of five, as well as rather high temperatures (Mayer et al. 2003). Fossil bones fulfill these requirements for the formation of Mn^{5+} apatites. They are composed of non-stoichiometric poorly crystalline apatite, often presenting an excess of Ca due to secondary diagenetically formed calcite and traces of Mn. The Mn^{5+} oxidation state is strongly stabilized if an "un-occupied" tetrahedral site in the apatite structure is offered. Otherwise, Mn will enter the Ca^{2+} position as Mn^{2+} and the apatite will not show a blue coloration. Generally, the polygonal bone apatite crystal shape and sizes of some hundreds of nanometers as well as the blue color due to Mn^{5+} ions of bones can be used as an unambiguous marker of a heating process.

ACKNOWLEDGMENTS

The authors (C.C., C.V., and I.R.) acknowledge Christian Brouder from the Institut de Minéralogie et de Physique des Milieux Condensés (IMPMC) for his help during UV/Visible/near-IR reflectance analyses. They thank the AGLAE team, especially Joseph Salomon and Laurent Pichon for their help during work at the accelerator. Françoise Pillier is acknowledged for her support during TEM analysis. Yves Adda is thanked for the fruitful discussions. GDR 2114 CNRS Chimart 2 is thanked for financial support of the project. The junior authors (J.A.C. and E.J.) acknowledge the support from the National Geographic Society, National Speleological Society, Geological Society of America, American Society of Mammalogists, Cave Research Foundation, and the Museum of Texas Tech University for excavation and research at San Josecito Cave. The federal Mexican founding agency CONACYT is acknowledged by J.A.C. for its support of his doctoral studies that included the excavation of the cave. This manuscript represents part of the ongoing Lubbock Lake Landmark Quaternary regional research program on the paleoecology and taphonomy of the Southern Plains. In addition, we thank the two reveiwers and E. Libowitzky for constructive reviews of the manuscript.

REFERENCES CITED

Arroyo-Cabrales, J. and Johnson, E. (1998) La Cueva de San Josecito, Nuevo León, México: Una primera interpretación paleoambiental. Universidad Autónoma del Estado de Hidalgo, Instituto de Investigaciones en Ciencias de la Tierra, Publicación Especial, 1, 120–126.

Calligaro, T., Dran, J.-C., Salomon, J., and Walter, P. (2004) Review of accelerator gadgets for art and archaeology. Nuclear Instruments and Methods in Physics B, 226, 29–37.

Chalmin, E., Vignaud, C., Farges, F., and Menu, M. (2008) Heating effect on manganese oxides used as black Paleolithic pigment. Phase Transitions, 81, 179–203.

Dardenne, K., Vivien, D., and Huguenin, D. (1999) Color of Mn(V)-Substituted Apatites $A_{10}[(B, Mn)O_4]_6F_2$, A= Ba, Sr, Ca; B = P, V. Journal of Solid State Chemistry, 146, 464–472.

Gonzalez, S., Jiménez-López, J.C., Hedges, R., Huddart, D., Ohman, J.C., and Pompa y Padilla, J.A. (2003) Earliest humans in the Americas: new evidence from México. Journal of Human Evolution, 44, 379–387.

Leventouri, T. (2006) Synthetic and biological hydroxyapatites: Crystal structure questions. Biomaterials, 27, 3339–3342.

Maxwell, J.A., Campbell, J.L., and Teedsdale, W.J. (1988) The Guelph PIXE Software. A description of the code package. Nuclear Instruments and Methods in Physics B, 43, 218–230.

Mayer, I., Jacobsohn, O., Niazov, T., Werckman, J., Iliescu, M., Richard-Plouet, M., Burghaus, O., and Reinen, D. (2003) Manganese in precipitated hydroxyapatites. European Journal of Inorganic Chemistry, 7, 1445–1451.

Michel, V., Bocherens, H., Théry-Parisot, I., Valoch, K., and Valensi, P. (2006) Colouring and preservation state of faunal remains from the Neanderthal levels of Kulna Cave, Czech Republic. Geoarcheology: An International Journal, 21, 479–501.

Reiche, I. and Chalmin, E. (2008) Synchrotron radiation and cultural heritage: combined XANES/XRF study at Mn *K*-edge of blue, grey or black coloured palaeontological and archaeological bone material. Journal of Analytical Atomic Spectrometry, 23, 799–806.

Reiche, I., Vignaud, C., and Menu, M. (2000) Heat-induced transformation of fossil mastodon ivory into "odontolite." Structural and elemental characterisation. Solid State Science, 2, 625–636.

Reiche, I., Vignaud, C., Champagnon, B., Panczer, G., Brouder, C., Morin, G., Solé, V.A., Charlet, L., and Menu, M. (2001) From mastodon ivory to gemstone: The origin of turquoise color in odontolite. American Mineralogist, 86, 1519–1524.

Reiche, I., Morin, G., Brouder, C., Solé, V.A., Petit, P.E., Vignaud, C., Calligaro, T., and Menu, M. (2002a) Manganese accomodation in fossilised mastodon ivory and heat-induced colour transformation: Evidence by EXAFS. European Journal of Mineralogy, 14, 1069–1073.

Reiche, I., Vignaud, C., and Menu, M. (2002b) The crystallinity of ancient bone and dentine: New insights by transmission electron microscopy. Archaeometry, 44, 447–459.

Reiche, I., Favre-Quattropani, L., Vignaud, C., Bocherens, H., Charlet, L., and Menu, M. (2003) A multi-analytical study of bone diagenesis: the Neolithic site of Bercy (Paris, France). Measurement Science and Technology, 14, 1608–1619.

Reiche, I., Chadefaux, C., Vignaud, C., and Menu, M. (2007) Les matériaux osseux archéologiques Des biomatériaux nanocomposites complexes. L'actualité Chimique, 312–313, 86–92.

Reinen, D., Lachwa, H., and Allmann, R. (1986) EPR- und ligandenfeldspektroskopische Untersuchungen an Mn^{V}-haltigen Apatiten sowie die Struktur von $Ba_5(MnO_4)_3Cl$. Zeitschrift für Anorganische und Allgemeine Chemie, 542, 71–88.

Robles, J., Arroyo-Cabrales, J., Johnson, E., Allen, B.L., and Izquierdo, G. (2002) Blue bone analyses as a contribution to the study of bone taphonomy in San Josecito Cave, Nuevo Leon, Mexico. Journal of Cave and Karst Studies, 64, 145–149.

Susini, J., Salomé, M., Fayard, B., Ortega, R., and Kaulich, B. (2002) The scanning X-ray microprobe at the ESRF X-ray microscopy beamline. Surface Reviews Letters, 9, 203–211.

Taniguchi, Y., Hirao, Y., Shimadzu, Y., and Tsuneki, A. (2002) The first fake? Imitation turquoise beads recovered from a Syrian neolithic site, Tell El-Kerkh. Studies in Conservation, 47, 175–183.

Tuross, N., Behrensmeyer, A.K., and Eanes, E.D. (1989) Strontium increases and crystallinity changes in taphonomic and archaeological bone. Journal of Archaeological Science, 16, 661–672.

Weiner, S. and Bar-Yosef, O. (1990) States of preservation of bones from prehistoric sites in the Near East: A survey. Journal of Archaeological Science, 17, 187–196.

Weiner, S., Quinqi, X., Goldberg, P., Jinyi, L., and Bar-Yosef, O. (1998) Evidence for the use of fire at Zhoukoudian, China. Science, 281, 251–253.

Winterer, M. (1997) XAFS: A data analysis program for materials science. Journal de Physique IV France, 7, 243–244.

Yubao, L., Klein, C.P.A.T., Zhang, X.D., and de Groot, K. (1993) Relationship between the colour change of hydroxyapatite and the trace element manganese. Biomaterials, 14, 969–972.

Manuscript received November 14, 2007
Manuscript accepted July 24, 2008
Manuscript handled by Eugen Libowitzky